

Article

Studies on Multi-Constraints Cooperative Guidance Method Based on Distributed MPC for Multi-Missiles

Mingyu Cong ^{1,2,3}, **Xianghong Cheng** ^{1,2,*} , **Zhiqian Zhao** ³ and **Zhijun Li** ³¹ School of Instrument Science & Engineering, Southeast University, Nanjing 210096, China; 230188067@seu.edu.cn² Key Laboratory of Micro-Inertial Instrument and Advanced Navigation Technology, Ministry of Education, Southeast University, Nanjing 210096, China³ Jiangxi Hongdu Aviation Industry Group, Nanchang 330024, China; airlqbz@163.com (Z.Z.); lizhijunde@163.com (Z.L.)

* Correspondence: xhcheng@seu.edu.cn

Abstract: Cooperative terminal guidance with impact angle constraint is a key technology to achieve a saturation attack and improve combat effectiveness. The present study envisaged cooperative terminal guidance with impact angle constraint for multiple missiles. In this pursuit, initially, the three-dimensional cooperative terminal guidance law with multiple constraints was studied. The impact time cooperative strategy of virtual leader missile and follower missiles was designed by introducing virtual leader missiles. Subsequently, based on the distributed model prediction control combined with the particle swarm optimization algorithm, a cooperative terminal guidance algorithm was designed for multiple missiles with impact angle constraint that met the guidance accuracy. Finally, the effectiveness of the algorithm was verified using simulation experiments.



Citation: Cong, M.; Cheng, X.; Zhao, Z.; Li, Z. Studies on Multi-Constraints Cooperative Guidance Method Based on Distributed MPC for Multi-Missiles. *Appl. Sci.* **2021**, *11*, 10857. <https://doi.org/10.3390/app112210857>

Academic Editors: Wei Huang and Dong Zhang

Received: 18 October 2021

Accepted: 8 November 2021

Published: 17 November 2021

Publisher's Note: MDPI stays neutral with regard to jurisdictional claims in published maps and institutional affiliations.



Copyright: © 2021 by the authors. Licensee MDPI, Basel, Switzerland. This article is an open access article distributed under the terms and conditions of the Creative Commons Attribution (CC BY) license (<https://creativecommons.org/licenses/by/4.0/>).

1. Introduction

Cooperative guidance is one of the key technologies for multiple missiles to attack and intercept large maneuvering targets with a high accuracy [1,2]. The two major types of cooperative guidance technology that have been extensively studied include independent cooperative guidance and distributed cooperative guidance.

Independent cooperative guidance determines the main guidance information by relying on only its own individual information, and there is no interaction of information between the missiles. The attack tasks are completed independently according to the designated guidance law and impact time before the launch. Wu S.T. et al. [3] was the first to propose the guidance problem along with the impact time. After more than ten years of development, many research results have emerged in this field. Based on the combination of the optimal control and time adjustment, Ma G.X. et al. [4] designed a cooperative guidance law with the impact time and angle constraints, and realized the cooperative interception based on the impact angle constraints. Li G.Y. et al. [5] designed the cooperative guidance law for multiple missiles based on the terminal sliding mode control method and the principle of consistency. They obtained the line-of-sight (LOS) angle rate for all the cooperative missiles converging to zero in a finite time, and it was found that the LOS angle converged to the desired angle. Zhou J. et al. [6] proposed a cooperative guidance law based on “leader-follower” architecture and sliding mode control to achieve a cooperative attack with line-of-sight (LOS) angle constraints on moving targets. Based on the impact angle, a guidance law with the impact time based on the sliding mode control was designed [7,8]. During the flight, multiple missiles exchange information with each other, “negotiate” together, and adjust their impact time according

to a certain strategy in order to achieve simultaneous arrival and saturation attack. This is called distributed cooperative guidance. Various studies that have been conducted on distributed cooperative guidance includes the time cooperative guidance law based on bias proportional guidance, the time cooperative guidance law based on the leader-follower and the time based on switching logic. Using a weighted average consensus algorithm, a distributed time cooperative guidance law was designed [9,10]. Wang X. et al. [11] designed the guidance law with the impact time based on a bias proportional guidance. Assuming that each missile had the same speed, Tekin R. et al. [12] designed a time cooperative guidance law based on the ‘leader-follower’ model. Jeon J.S. et al. [13] considered the integration of the time cooperative guidance and control and studied the tracking problem of the nominal projectile distance.

The guidance law with impact time constraints is a key technology in achieving saturation attack, break through anti-missile defense systems, and accomplishing reliable strikes against important strategic targets. Lin D.F. et al. [14] designed a cooperative guidance law with an impact time control and field of view constraints of the seeker for the cooperative guidance of multiple missiles in attacking low-speed targets. Li G.Y. et al. [15] designed the cooperative guidance law for multiple missiles to simultaneously intercept high maneuvering targets and designed the cooperative guidance law for multiple missiles based on the terminal sliding mode control method and the principle of consistency to achieve the LOS angle rate of the cooperative missiles converging to zero in a finite time. In view of the Field of View (FOV) constraints of the missiles, the terminal LOS angle constraints [16–18] were employed in the design of the cooperative guidance law, along with the impact time constraints.

Considering the research on the cooperative guidance algorithm, there are more studies on the guidance law with impact angle or time constraints [19–26], and relatively fewer studies on combining the two as terminal constraints [27–31]. Impact time constraints are the basis of the cooperative guidance algorithm and are indispensable. Impact angle constraints can make the missile hit the target with the best attitude in order to maximize the effectiveness of the warhead to achieve a maximum damage. Hence, considering both impact time and impact angle constraints in the cooperative terminal guidance algorithm is of great significance for improving the effective damage and combat capability of the cruise missile weapon system.

Model prediction control (MPC), also known as receding horizon control (RHC), has an online rolling optimization at the core, which is essentially an optimal control problem in the finite time domain. At each optimal control moment, the current optimal control domain can be obtained, and the first part of the domain is used as the optimal control to act on the system. The optimal control sequence is obtained after multiple sampling. MPC is a model-based algorithm that has been widely used in industry, metallurgy, etc. [32]. In recent years, MPC has been continuously improved, and a few improved methods have been proposed for MPC [33–36], which achieved better application prospects and obtained better prediction results.

In the present study, we proposed a three-dimensional cooperative terminal guidance law that met the constraints of impact angle and impact time simultaneously, on the premise of meeting the requirements of miss distance. First, the nonlinear motion model of the missile and the target was established, the state quantity and the control quantity were normalized, the concept of leader-follower missiles was introduced, and the impact time cooperative strategy of leader and follower missiles was designed. Subsequently, based on the model predictive control method, a three-dimensional cooperative terminal guidance law was proposed that simultaneously controlled multiple missiles to perform attacks on the target with the constraints of impact time and impact angle on the premise of meeting the requirements of miss distance. Finally, by introducing one leader missile and four follower missiles to simulate the multi-missile cooperative attack against stationary targets, linear moving targets, and snake-shaped maneuvering targets, the effectiveness of the multi-constraint cooperative guidance law algorithm was verified.

2. Description of Cooperative 3D Terminal Guidance for Multiple Missiles

The relative motion relationship between the missile and the target is shown in Figure 1. Herein, M and T represent the missile and the target, respectively. The ground inertial coordinate system is expressed in the A-XYZ plane. This is the relative distance between the missile and the target, is the line-of-sight elevation angle and the line-of-sight azimuth angle, represents the trajectory inclination angle and the trajectory deflection angle of the missile, and represents the trajectory inclination angle and the trajectory deflection angle of the target. Unless otherwise specified, all angles were positive counterclockwise.

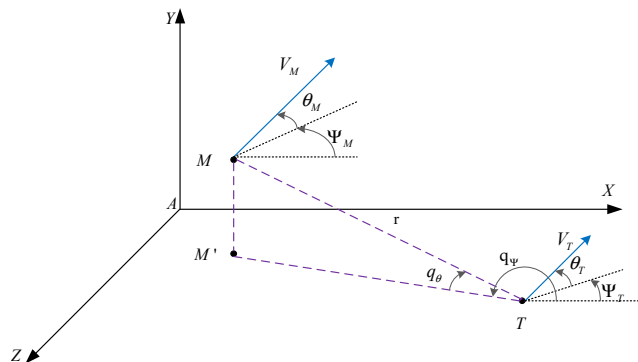


Figure 1. Guidance geometric relationship.

According to the relative geometric relationship between the missile and the target in Figure 1, the relative motion can be obtained as:

$$\left\{ \begin{array}{l} \frac{dL}{dt} = \frac{d}{dt}(r\mathbf{i}_L) = \mathbf{V}_T\mathbf{i}_T - \mathbf{V}_M\mathbf{i}_M = \dot{r}\mathbf{i}_L + \boldsymbol{\Omega}_L \times r\mathbf{i}_L \\ \mathbf{A}_T = A_{yt}\mathbf{j}_T + A_{zt}\mathbf{k}_T = \boldsymbol{\Omega}_L \times \mathbf{V}_T + \boldsymbol{\Omega}_T \times \mathbf{V}_T \\ \mathbf{A}_M = A_{ym}\mathbf{j}_M + A_{zm}\mathbf{k}_M = \boldsymbol{\Omega}_L \times \mathbf{V}_M + \boldsymbol{\Omega}_M \times \mathbf{V}_M \\ \boldsymbol{\Omega}_L = \dot{\psi}_L \sin \theta_L \mathbf{i}_L - \dot{\theta}_L \mathbf{j}_L + \dot{\psi}_L \cos \theta_L \mathbf{k}_L = \dot{\lambda}_x \mathbf{i}_L + \dot{\lambda}_y \mathbf{j}_L + \dot{\lambda}_z \mathbf{k}_L \\ \boldsymbol{\Omega}_M = \dot{\psi}_m \sin \theta_m \mathbf{i}_M - \dot{\theta}_m \mathbf{j}_M + \dot{\psi}_m \cos \theta_m \mathbf{k}_M \\ \boldsymbol{\Omega}_T = \dot{\psi}_t \sin \theta_t \mathbf{i}_T - \dot{\theta}_t \mathbf{j}_T + \dot{\psi}_t \cos \theta_t \mathbf{k}_T \end{array} \right. \quad (1)$$

where \mathbf{V}_T and \mathbf{V}_M are the velocity vectors of the target and the missile, respectively; A_{zm} and A_{ym} are the normal accelerations of the turning plane and the dive plane of the missile, respectively; A_{zt} and A_{yt} are the normal accelerations of the target turning plane and the dive plane, respectively; $\boldsymbol{\Omega}_L$ is the rotation angular velocity vector of the line-of-sight coordinate system; $\boldsymbol{\Omega}_T$ is the rotation angular velocity vector of the target relative to the line of sight coordinate system; and $\boldsymbol{\Omega}_M$ is the rotation angular velocity vector of the missile relative to the line of sight coordinate system.

From Equation (1), the following differential equations can be obtained:

$$\left\{ \begin{array}{l} \dot{r} = V_m \cdot (\rho \cos \theta_t \cos \psi_t - \cos \theta_m \cos \psi_m) \\ r\dot{\lambda}_y = V_m \cdot (\sin \theta_m - \rho \sin \theta_t) \\ r\dot{\lambda}_z = V_m \cdot (\rho \cos \theta_t \sin \psi_t - \cos \theta_m \sin \psi_m) \\ \dot{\theta}_m = \frac{A_{zm}}{V_m} + \frac{1}{r} V_m \tan \lambda_y \sin \psi_m (\rho \cos \theta_t \sin \psi_t - \cos \theta_m \sin \psi_m) - \frac{1}{r} V_m \cos \psi_m (\rho \sin \theta_t - \sin \theta_m) \\ \dot{\psi}_m = \frac{A_{ym}}{V_m \cos \theta_m} - \frac{1}{r \cos \theta_m} V_m \sin \theta_m \cos \psi_m \times \tan \lambda_y (\rho \cos \theta_t \sin \psi_t - \cos \theta_m \sin \psi_m) \dots \\ - \frac{1}{r \cos \theta_m} V_m \sin \theta_m \sin \psi_m (\rho \sin \theta_t - \sin \theta_m) - \frac{1}{r} V_m (\rho \cos \theta_t \sin \psi_t - \cos \theta_m \sin \psi_m) \\ \dot{\theta}_t = \frac{A_{zt}}{V_t} + \frac{1}{r} V_m \sin \psi_t \tan \lambda_y (\rho \cos \theta_t \sin \psi_t - \cos \theta_m \sin \psi_m) - \frac{1}{r} V_m \cos \psi_t (\rho \sin \theta_t - \sin \theta_m) \end{array} \right. \quad (2)$$

where $\rho = V_t / V_m$ is the speed ratio of the target relative to the missile; \mathbf{A}_M and \mathbf{A}_T are the acceleration vectors of the missile and the target, respectively; and A_{zmd} and A_{ynd} are the acceleration commands for the longitudinal and lateral channels of the missile, respectively.

3. Strategy for Timed Cooperative Guidance of Multiple Missiles

For cooperative guidance, one of the important features is the ability wherein the multiple missiles can hit the target simultaneously. In order to achieve this goal, the present study employed the concept of virtual leader missile. According to the selection principle, one of the missiles was selected as the virtual leader missile, and the traditional guidance scheme was adopted to make it fly towards the target, while the remaining missiles were regarded as follower missiles. In the dive plane, the follower missiles used the same guidance algorithm as the virtual leader missile. In the turning plane, the follower missiles realized the time cooperation through lateral maneuvering (which was mainly achieved by controlling the relative distance between the missile and the target).

3.1. Movement Law of the Virtual Leader Missile

The relative motion relationship of the leader-follower missiles can be seen from Figure 2. Considering that Missiles Leader (ML) is the leader missile, M_i is the i th follower missile, and T is the target, the velocity of the leader missile is V_{m0} , the trajectory inclination angle and the trajectory deflection angle are θ_0 and ψ_0 , respectively; the vertical and azimuth LOS angle are θ_{0L} and ψ_{0L} , respectively; the velocity of the i th follower missile is V_{mi} ; the trajectory inclination angle and the trajectory deflection angle are θ_i and ψ_i , respectively; and the vertical and azimuth LOS angles are θ_{0i} and ψ_{0i} , respectively.

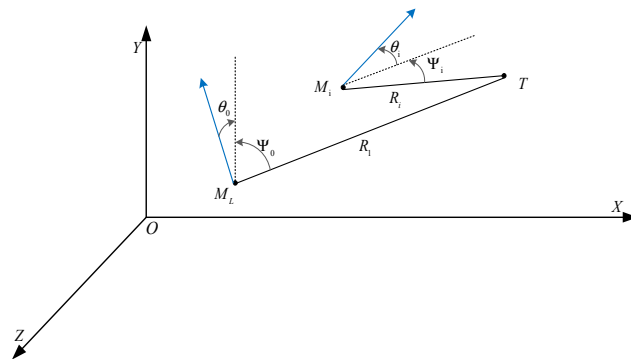


Figure 2. Relative motion relationship of the leader-follower missiles.

In the later stage of the missile movement, the guidance of the missiles makes θ_0 and θ_i tend to zero. At this time, the curvature of the trajectory curve of the leader missile and the follower missiles tends to be consistent, that is, the relationships $r_0/V_{m0} = r_i/V_{mi}$ and $\psi_0 = \psi_i$ (or $r_0/V_{m0} = r_i/V_{mi}$ and $\psi_0 = -\psi_i$) are satisfied, and the leader missile and follower missiles reach and hit the target simultaneously. The important aspect is that this strategy can make a same curvature of the leader missile and follower missiles relative to the velocity. Under this condition, the flight of the missile consumes the same time. Hence, the leader-follower strategy can also be suitable for different missile speeds. The leader missile adopts an augmented proportional guidance method as:

$$A_{z0} = K_{01} |\dot{r}_0| \theta_{L0} / \cos \theta_0 \quad (3)$$

$$A_{y0} = - \frac{K_{01} |r_0| \theta_{L0} \sin \theta_0 \sin \psi_0}{\cos \theta_0 \cos \psi_0} - \frac{K_{02} |r_0| \psi_{L0} \cos \theta_{L0}}{\cos \psi_0} \quad (4)$$

In order to quickly make the attitude angle θ_0 of the leader missile tend towards zero, a larger value of K_{01} needs to be chosen. The follower missiles also adopt an augmented proportional guidance method on the pitch channel:

$$A_{zi} = K_{i1} |\dot{r}_i| \theta_{Li} / \cos \theta_i \quad (5)$$

In order to quickly make the attitude angle θ_i of the leader missile tend towards zero, a larger value of K_{i1} needs to be chosen. Next, according to the position relationship between the leader missile and the follower missiles, the lateral acceleration A_{yi} of the leader missile is designed so that $r_i/V_{mi} \rightarrow r_0/V_{m0}$ and $\psi_i \rightarrow \pm\psi_0$ are satisfied during the guidance process.

3.2. Cooperative Strategy of Follower Missiles

The remaining time error between the leader missile and follower missiles is defined as follows:

$$\xi = \frac{r_0}{V_{m0}} - \frac{r_i}{V_{mi}} \quad (6)$$

By deriving the remaining time error with respect to time, we can get:

$$\dot{\xi} = \cos \theta_i \cos \psi_i - \cos \theta_0 \cos \psi_0 \quad (7)$$

According to Equation (7), A_{yi} indirectly controls ξ by controlling ψ_i . Therefore, the control system can be divided into two sub-control systems according to direct control ψ_i and indirect control ξ , namely, a nonlinear slow sub-system and a nonlinear fast sub-system. Therefore, the dynamic design method of time-scale separation is used to design the control instructions A_{yi} . The desired dynamics of the slow sub-system is expressed as:

$$\dot{\xi}_{des} = -K_R \xi \quad (8)$$

where K_R is the bandwidth of the slow sub-system.

If $\dot{\xi} = \dot{\xi}_{des}$ is obtained through the control, considering the command value of ψ_i is ψ_i^c , then:

$$\cos \psi_i^c = \frac{\cos \theta_0 \cos \psi_0 - K_R \xi}{\cos \theta_i} \quad (9)$$

Because the value range of ψ_i is $(-\pi/2, \pi/2)$, ψ_i^c is within the value range. Combining the above equation and the value range, the value range of K_R can be obtained:

$$\frac{\cos \theta_0 \cos \psi_0 - \cos \theta_i}{\xi} \leq K_R \leq \frac{\cos \theta_0 \cos \psi_0}{\xi} \quad (10)$$

if

$$K_R = \frac{\cos \theta_0 \cos \psi_0 - \cos \theta_i + c_1 \frac{\xi}{\xi + c_2} \cos \theta_i}{\xi} \quad (11)$$

where c_1, c_2 are constants and satisfy the relationship $0 < c_1, c_2 < 1$.

Herein, ψ_i^c can be expressed as:

$$\psi_i^c = f_\psi \times \arccos \left(\frac{\cos \theta_0 \cos \psi_0 - K_R \xi}{\cos \theta_i} \right) \quad (12)$$

where $\psi_i \in [-\pi/2, 0], f_\psi = -1; \psi_i \in [0, \pi/2], f_\psi = 1$.

Taking the derivative of Equation (12) with respect to time, we have:

$$\dot{\psi}_i^c = f_\psi \times \left(\begin{array}{l} K_R \cos \psi_i - \frac{\cos \psi_i^c \sin \theta_i}{\cos \theta_i} - \\ \frac{K_R \cos \theta_0 \cos \psi_0 - \dot{\theta}_0 \sin \theta_0 \cos \psi_0 - \dot{\psi}_0 \cos \theta_0 \sin \psi_0}{\cos \theta_i \sqrt{1 - (\cos \psi_i^c)^2}} \end{array} \right) \quad (13)$$

If $\psi_i \in [-\pi/2, 0], f_\psi = -1; \psi_i \in [0, \pi/2], f_\psi = 1$.

In order to make ξ satisfy the relation in Equation (8), ψ_i should quickly converge to near its command value ψ_i^c . Therefore, the following fast dynamics sub-system is designed, and its specific expression is given as:

$$\dot{\psi}_{i,des} - \dot{\psi}_i^c = -K_\psi(\psi_i - \psi_i^c) \quad (14)$$

where K_ψ is the bandwidth of the fast sub-system. Under the control $\dot{\psi}_i = \dot{\psi}_{i,des}$ united with Equation (4), the final designed maneuvering control command in the turning plane can be obtained as:

$$A_{yi} = \frac{V_{mi}^2}{r_i} \sin \psi_i (1 - \cos \theta_i \sin \theta_i \cos \psi_i \tan \theta_{Li}) - V_{mi} \cos \theta_i \dot{\psi}_i^c + K_\psi V_{mi} \cos \theta_i (\psi_i - \psi_i^c) \quad (15)$$

Equation (14) can be satisfied by maneuvering control commands on the lateral plane, so that $\psi_i \rightarrow \psi_i^c$ is obtained; ψ_i^c can make the slow dynamics sub-system meet Equation (8). Under this condition, the time cooperative control of multiple missiles can be realized. Longitudinal control commands A_{z0} and A_{zi} can make $\theta_0 \rightarrow 0$ and $\theta_i \rightarrow 0$, along with the control of the yaw channel, $\xi \rightarrow 0$, so as to realize $\psi_i \rightarrow \psi_0$ (or $\psi_i \rightarrow -\psi_0$). The control flow chart for cooperative guidance of multiple missiles can be seen from Figure 3.

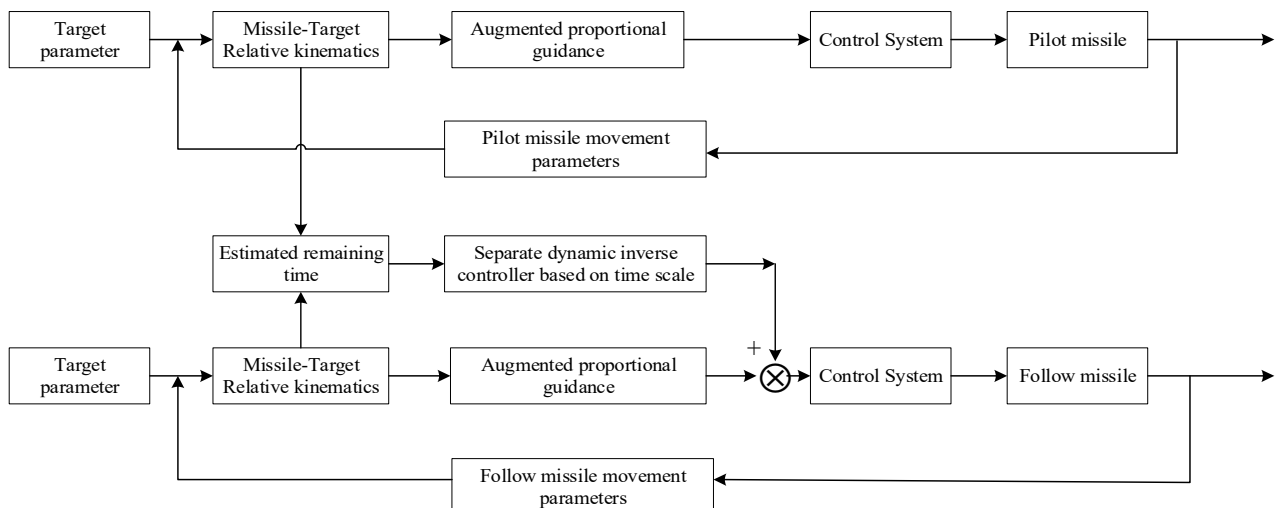


Figure 3. Control flow chart for cooperative guidance of multiple missiles.

4. Cooperative Prediction Guidance Based on Distributed Model Prediction Control (DMPC) for Multiple Missiles

4.1. Introduction to DMPC

The application of the MPC method in a multi-agent cluster system has three structures: centralized, decentralized, and distributed MPC. As shown in Figure 4, the centralized MPC considers the overall performance of the cluster as an optimization index. In each sampling period, a central model predictor performs the rolling optimization on the overall control performance index of the cluster system to obtain the control sequence set with the best overall performance of the cluster system. Each sub-system of the decentralized and distributed MPC has an independent model predictor, which reduces the dimensionality of the system. It also reduces the amount of calculation for the online optimization of each sub-controller and increases the reliability of the system. The difference between the distributed and decentralized MPC is that there is no information interaction between the sub-controllers of the decentralized MPC. As a result, it cannot control the problem of the multi-agent system with coupling between the sub-systems.

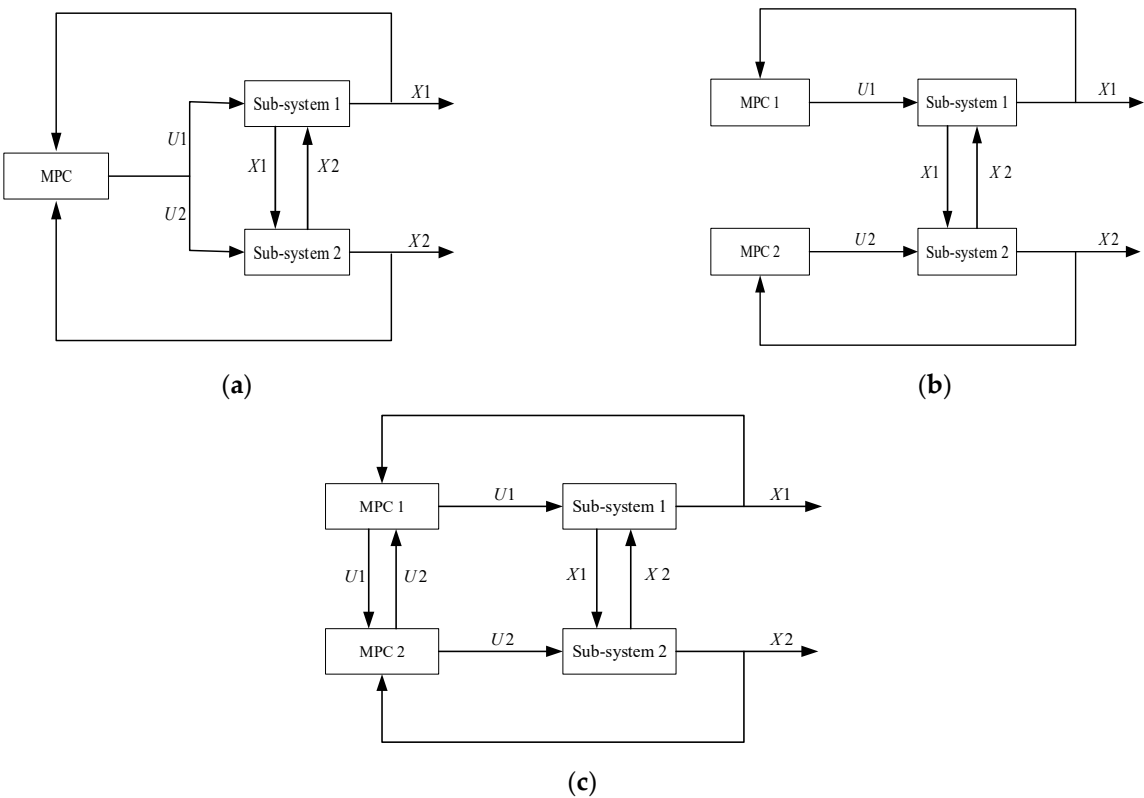


Figure 4. Classification of MPC: (a) Centralized MPC; (b) Decentralized MPC; (c) Distributed MPC.

From the above-mentioned missile motion model, the motion equation of each missile can be expressed as:

$$\dot{z}_i(t) = f_i(z_i(t), u_i(t)), t \geq t_0, z_i(0) = z_0 \quad (16)$$

Therefore, the motion equations of its adjacent missiles can be defined as follows:

$$\dot{z}_{-i}(t) = f_{-i}(z_{-i}(t), u_{-i}(t)), t \geq t_0 \quad (17)$$

The prediction time domain is defined as $T_p \in (0, \infty)$, $s \in [t_c, t_c + T_p]$. The control moment of the receding horizon control is defined as $t_c = t_0 + \delta_c$, $c \in \{0, 1, 2, \dots\}$, where δ is the control interval and satisfies $\delta \in (0, T_p]$, $\hat{z}_i(s; t_c)$, $\hat{u}_i(s; t_c)$ is the estimated state sequence and control sequence, respectively, while $z_i^p(s; t_c)$ and $u_i^p(s; t_c)$ are the predicted state sequence and control sequence, respectively. For any time, t_c , the optimal control sequence of the i th missile can be expressed as:

$$u_i^*(s; t_c) = \operatorname{argmin}_{u_i^*(s; t_c)} \mathcal{J}_i(z_i(s; t_c), z_{-i}(s; t_c), u_i(s; t_c)) \quad (18)$$

The cost function can be expressed as:

$$\mathcal{J}_i = \int_{t_c}^{t_c + T_p} F_i(z_i^p(s; t_c), \hat{z}_{-i}(s; t_c), u_i^p(s; t_c)) ds + \Phi_i(z_i^p(t_c + T_p; t_c)) \quad (19)$$

where \mathcal{J}_i is the operation function and Φ is the final state function. The following constraints are satisfied:

$$\dot{z}_i^p(s; t_c) = f_i(z_i^p(s; t_c), u_i^p(s; t_c)) \quad (20)$$

$$\dot{\hat{z}}_{-i}(s; t_c) = f_{-i}(\hat{z}_{-i}(s; t_c), \hat{u}_{-i}(s; t_c)) \quad (21)$$

$$z_i^p(s; t_c), \hat{z}_{-i}(s; t_c) \in Z \quad (22)$$

$$u_i^p(s; t_c), \hat{u}_{-i}(s; t_c) \in U \quad (23)$$

According to the definition of the motion equations of the adjacent missiles, $s \in [t_c, t_c + T_p]$ in the prediction time domain and the estimated control sequence $\hat{u}_{-i}(s; t_c)$ can be obtained by:

$$\hat{u}_{-i}(s; t_c) = \{\hat{u}_j(s; t_c)\}, j \in N_i \quad (24)$$

In the prediction time domain $s \in [t_c, t_c + T_p]$, the estimated control sequence $\hat{u}_j(s; t_c)$ consists of two parts. In the time domain $s \in [t_c, t_{c-1} + T_p]$, the first part is the optimal control sequence $u_j^*(s; t_c)$ of the previous prediction time domain $s \in [t_{c-1}, t_{c-1} + T_p]$, while in the time domain $s \in [t_{c-1} + T_p, t_c + T_p]$, the second part is the optimal control sequence derived from $u_j^*(s; t_{c-1})$ at the time $s = t_{c-1} + T_p$. The expression of $\hat{u}_j(s; t_c)$ is as follows:

$$\hat{u}_j(s; t_c) = \begin{cases} u_j^*(s; t_{c-1}) & s \in [t_c, t_{c-1} + T_p] \\ u_j^*(t_{c-1} + T_p; t_{c-1}) & s \in [t_{c-1} + T_p, t_c + T_p] \end{cases} \quad (25)$$

4.2. Algorithm for Cooperative Guidance Considering Impact Time and Angle Constraints

The framework idea of the distributed MPC is as follows: At each control moment t_c , the current missile control variable is initialized with the optimal control amount of the previous prediction period $[t_{c-1}, t_{c-1} + T_p]$. After that, it exchanges the information with the adjacent missiles and receives the estimated value of the control variable at the moment t_{c-1} . Subsequently, it sends out the estimated value of its own control variable at the moment t_{c-1} to estimate the state of the adjacent missile in the prediction period $[t_c, t_c + T_p]$ and evaluates the cost function \mathcal{J}_i in the prediction period $[t_c, t_c + T_p]$ and uses the particle swarm optimization (PSO) algorithm to solve the optimal control variable sequence in the prediction period $[t_c, t_c + T_p]$. Based on the rolling optimization idea, the optimal control amount of the first update interval is taken to obtain the optimal control sequence, and the missile state at $[t_c, t_{c+1}]$ is updated to enter the next control moment t_{c+1} . The solution process of the estimated value is shown in Figure 5.

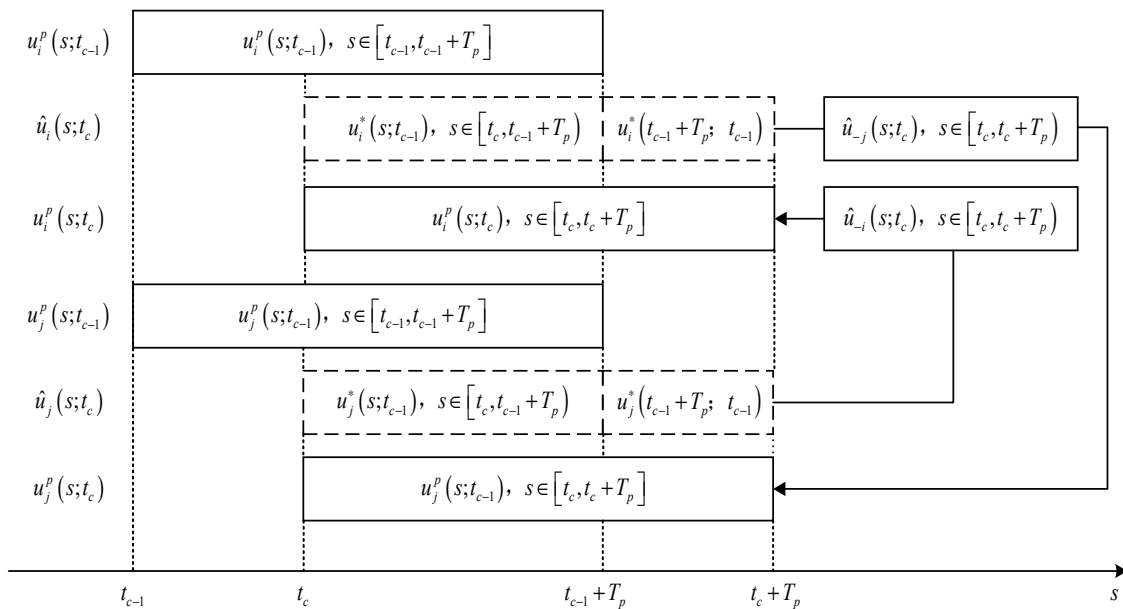


Figure 5. Solution process of the predicted state value.

The basic principle of the PSO-based distributed cooperative model prediction framework for multiple missiles is shown in Figure 6. The cost function of the cooperative

control of missiles includes two parts, namely, the operation function, F , and the final state function, Φ :

$$J_i = \int_{t_c}^{t_c+T_p} F_i(z_i^p(s; t_c), \hat{z}_{-i}(s; t_c), u_i^p(s; t_c)) ds + \Phi_i(z_i^p(t_c + T_p; t_c)) \quad (26)$$

The operation function is defined as:

$$F_i(z_i^p(s; t_c), \hat{z}_{-i}(s; t_c), u_i^p(s; t_c)) = \alpha \sum_{j \in N_i} \|t_{go,j}^p(s; t_c) - \hat{t}_{go,j}(s; t_c)\|^2 + (1 - \alpha) \|u_i^p(s; t_c)\|^2 \quad (27)$$

The final state function is defined as:

$$\Phi_i(z_i^p(t_c + T_p; t_c)) = \beta \|r_i(t_c + T_p; t_c)\|^2 + \gamma \|\theta(t_c + T_p; t_c) - \theta_{expect}\| + \|\psi(t_c + T_p; t_c) - \psi_{expect}\| \quad (28)$$

where α, β, γ are the weight constants, $\|\cdot\|$ represents the modulus of the space vector, N_i is the set of missiles other than missile i , r_i is the distance between the missile and the target, $t_{go,i}^p$ is the predicted time of arrival, and $\hat{t}_{go,i}$ is the estimated time of arrival, which can be solved by the following equation:

$$\hat{t}_{go,j}(s; t_c) = \frac{\hat{r}(s; t_c)}{v_j}, j \in N_i \quad (29)$$

where $\hat{r}(s; t_c)$ is the estimated distance between the missile and the target at the moment t_c , θ_{expect} and ψ_{expect} represent the desired pitch angle and trajectory deflection angle that are used to control the angle of the missile at the terminal landing point to achieve the impact angle constraints.

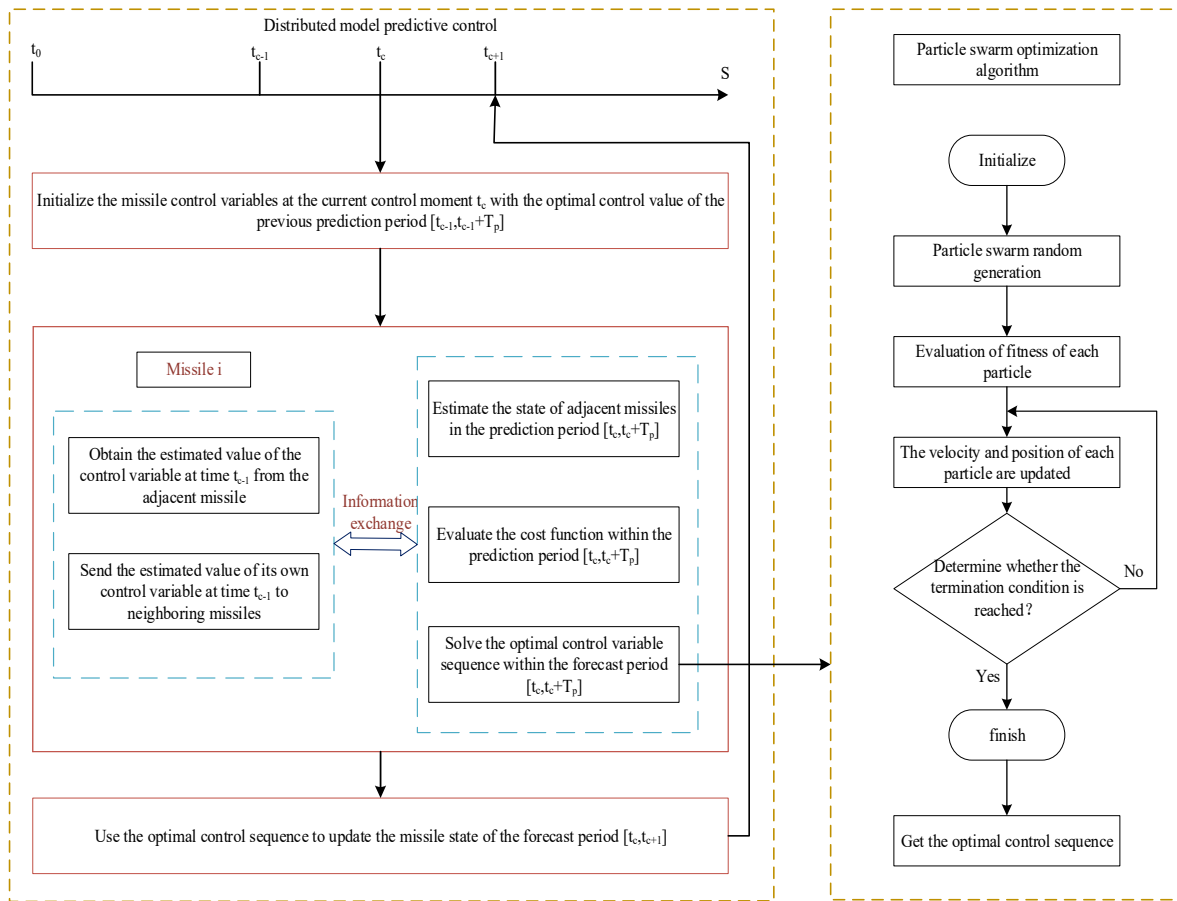


Figure 6. PSO-DMPC model prediction framework.

5. Verification by Simulations

Let M1, M2, M3, and M4 denote four missiles participating in cooperative operations. The target is in the horizontal plane, and its initial position is at the origin of the coordinates. Table 1 lists the initial parameters of the proposed virtual leader missile (denoted as M) and follower missiles.

Table 1. Initial parameters of the virtual leader and the follower missiles.

Name	Initial Position			Velocity	Ballistic Angle	Ballistic Drift Angle
Variable	x	y	z	Vm	θ	ψ
Unit	m	m	m	m/s	(°)	(°)
Virtual Pilot Missile	4000	1800	3000	133	45	45
M1	-3000	1500	-3800	155	45	45
Follow Missile	M2	-3500	1200	-2500	140	40
M3	3500	800	2000	125	10	30
M4	-3500	1600	2500	140	-15	20

Let us consider a case where a stationary target, a straight moving target, and a snake-like maneuvering target is attacked (specific movement of the target is shown in Table 2).

Table 2. Initial parameters of the virtual leader missile and follower missiles.

Type	Target Motion State		
Target 1		Static target	
Target 2	$v_t = 10 \text{ m/s}$	$a_t = 0 \text{ m/s}^2$	$\psi_{vt} = 45^\circ$
Target 3	$v_t = 10 \text{ m/s}$	$y_t = 60 \sin(x_t/100)$	$K_{01} = K_{i1} = 10$

The control coefficients of the augmented proportional guidance method adopted by the five missiles are $K_{01} = K_{i1} = 10$, $K_{02} = 5$; the parameters are $c_1 = 0.7$, $c_2 = 0.9$; the bandwidth of the fast dynamics sub-system is $K_\psi = 5$; and the overload limit of the missile is 8 g. The impact time during the attack on a fixed target is shown in Table 3. According to the above design strategy, under the premise of adopting the augmented proportional guidance method, the impact time of the leader missile is greater than that of each follower missile. Therefore, the use of this scheme can provide a sufficient flight time adjustment margin for the follower missiles.

Table 3. Impact time of APN guidance.

Target Type	Virtual Pilot Missile			Follow Missile		
	Unit	M	M1	M2	M3	M4
Target 1	s	41.66	33.92	32.85	33.25	32.93
Target 2	s	39.48	41.36	36.58	33.39	36.54
Target 3	s	39.82	39.95	34.67	34.01	35.31

In the adjustable range, in order to enhance the ability of attack and damage on moving targets in a horizontal plane, the ideal impact angles (θ_m^* , ψ_{vm}^*) of M1, M2, M3, and M4 are designated as $(50^\circ, -20^\circ)$, $(44^\circ, -34^\circ)$, $(-30^\circ, 0^\circ)$, and $(35^\circ, -20^\circ)$, respectively. The ideal impact time t^* is determined based on the flight time of the leader missile attacking different targets. The simulation results of cooperative attack by missiles on targets 1, 2, and 3 are shown in Figures 7–11.

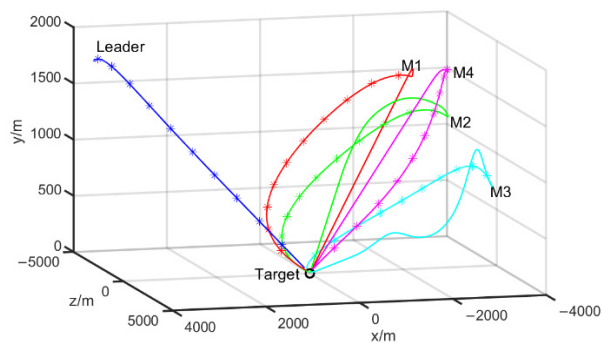


Figure 7. Flight trajectory curve of the cooperative attack on stationary target 1.

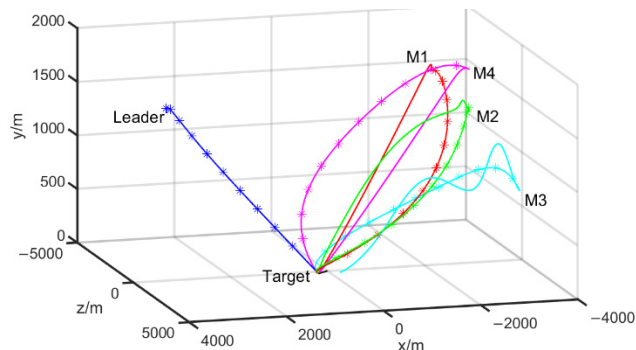


Figure 8. Flight trajectory curve of the cooperative attack on target 2.

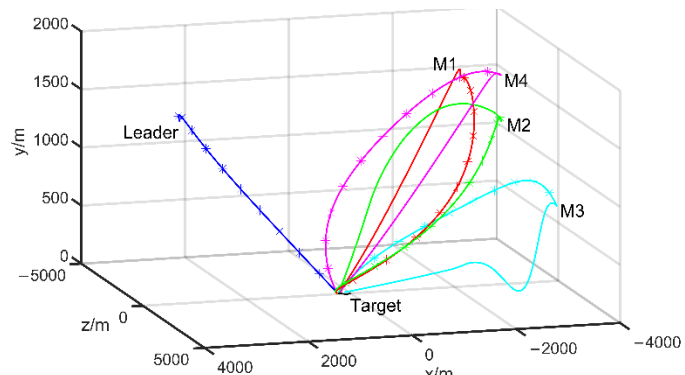


Figure 9. Flight trajectory curve of the cooperative attack on target 3.

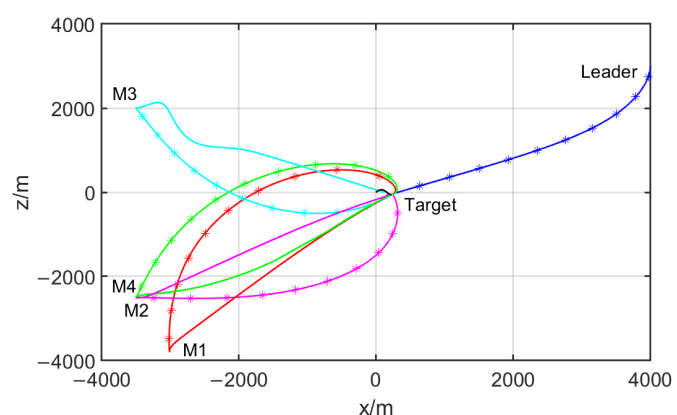


Figure 10. Projection of flight trajectory curve of cooperative attack on target 3 in the XOZ plane.

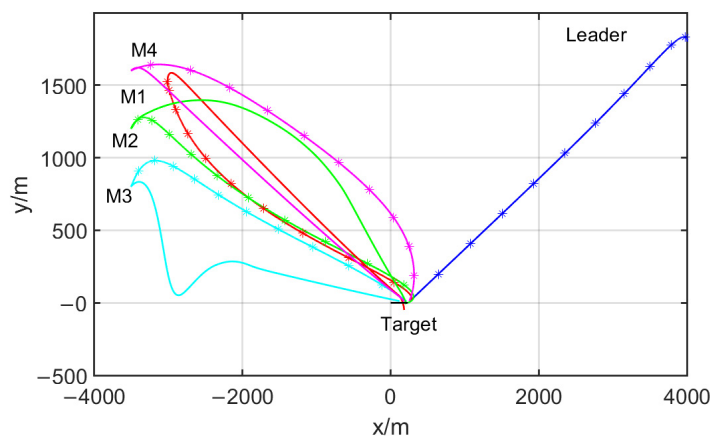


Figure 11. Projection of flight trajectory curve of cooperative attack on target 3 in the XOY plane.

As shown in Figures 7–9, the cooperative strategy based on the tracking of the missile-target distance could well constrain the missile-target distance during the flight of multiple projectiles. As a result, the follower missiles converged to the same value as the leader missile. The MPC-based cooperative guidance algorithm optimizes the trajectory to meet the terminal impact angle constraints, based on the impact time of the cooperative missile group. From Figures 10 and 11, it can be observed that the MPC-based cooperative guidance law can make multiple missiles participating in cooperative operations hit the target with separately specified impact angles at a specified time. The miss distance meets the requirements and is less than that of the cooperative time guidance. Additionally, the strike effect is more accurate. Due to the limited adjustable time and angle of the missiles under different position conditions, the omni-directional saturation attack of the multiple missiles can be realized through reasonable state estimation, mission planning, and assignment of multiple terminal guidance missiles. The simulation results verified the effectiveness of this method in attacking the stationary and maneuvering targets. From Figures 7–10, it can be observed that the trajectory curve optimized by the MPC algorithm is smoother and easier to implement.

By tracking the distance between the missile and the target, each follower missile achieved a cooperative impact time with the virtual leader missile. When hitting target 1, target 2, and target 3, the cooperative impact time of the four missiles was the same as the impact time of the virtual lead missile, which was 41.66 s, 41.28 s, and 41.82 s, respectively. However, the impact angle did not meet the requirements at this time, and the iterative optimization of the guidance instructions through the MPC algorithm achieved the impact angle constraints at the terminal. In the simulation example, the impact angle constrained by each follower missile and the terminal impact angle are given by Figures 12–14, when different guidance methods were used to attack an unfixed target.

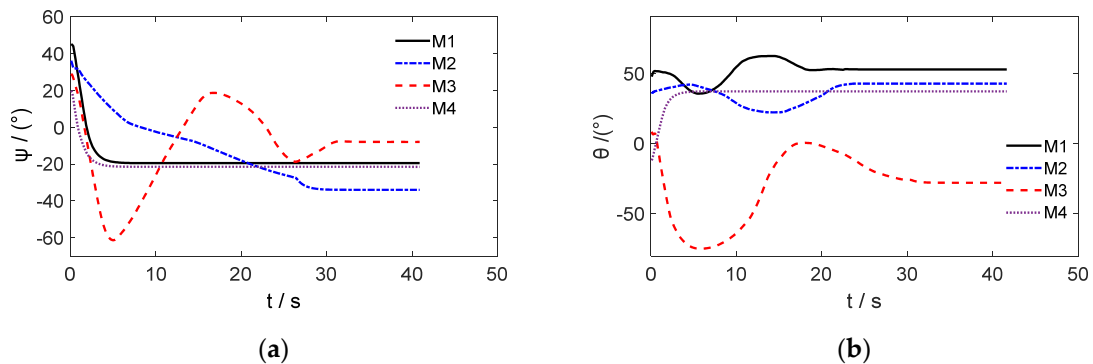


Figure 12. Velocity-inclination change curve of each follower missile during the cooperative attack on target 1 based on the MPC method: (a) Trajectory deflection curve; (b) Trajectory inclination curve.

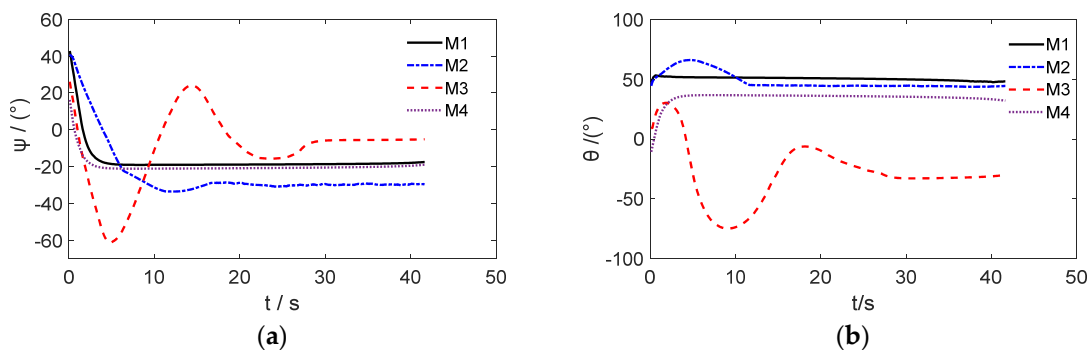


Figure 13. Velocity-inclination change curve of each follower missiles during cooperative attack on target 2 based on the MPC method: (a) Trajectory deflection curve; (b) Trajectory inclination curve.

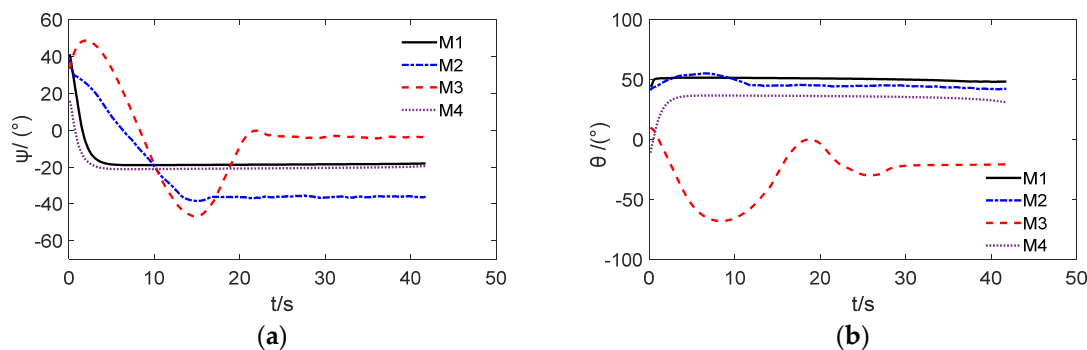


Figure 14. Velocity-inclination change curve of each follower missiles during the cooperative attack on target 3 based on the MPC method: (a) Trajectory deflection curve; (b) Trajectory inclination curve.

Figures 12–14 show the changing curves of the impact angle when attacking a stationary target, a uniformly moving target, and a maneuvering target by the MPC method. Using the MPC method can not only realize the cooperative time but can also satisfy the impact angle constraints. Both the time cooperative guidance and the MPC-based guidance can make four missiles hit the target at the same time, but the former could only constrain the impact time of four missiles, while the latter achieved a multi-directional cooperative attack with designated angles on the target. This verified the superior guidance performance of the MPC-based 3D cooperative guidance law with multiple constraints. Figure 15 shows the tracking curve of the missile-target distance in the time cooperative strategy with the designed parameters. Figure 16 shows the curve of the remaining time error with the time obtained by the MPC method. Tracking the missile-target distance of the leader missile achieves a cooperative impact time between the follower missles and the leader missile, but it does not meet the impact angle constraints. Therefore, the MPC method was used to iteratively optimize the control commands to meet the impact angle constraints.

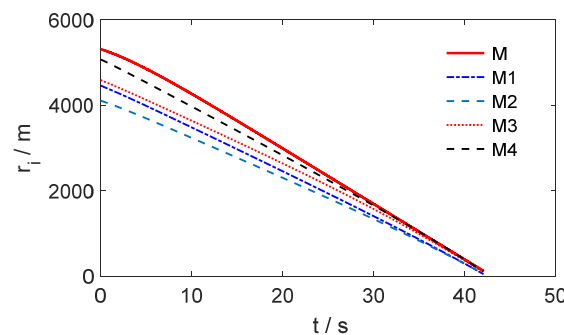


Figure 15. Tracking of the missile-target distance.

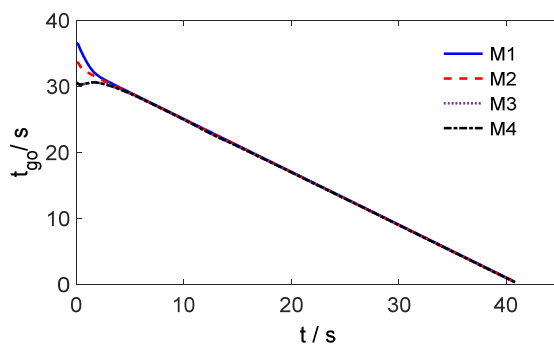


Figure 16. Remaining time error of MPC.

The performance of the MPC-based 3D cooperative guidance law and time cooperative guidance law are shown in Figures 17 and 18, respectively. It can be observed that, when the missile flies with the time cooperative guidance law, although the impact time was similar to the flight time of the leader missile, there was still a significant gap between the terminal attack attitude angle and the ideal impact angle. After iterative optimization using the MPC algorithm, both the trajectory inclination θ_{0L} and the trajectory deflection angle ψ_{0L} achieved the impact angle constraints within the specified time. The MPC algorithm is based on the principle of optimization and was designed according to performance indicators to minimize the total energy in the guidance process under the condition of meeting terminal constraints. In every iteration of the MPC algorithm, the deviation at the terminal of the trajectory was evenly distributed to each step of the entire trajectory by a controlled adjustment. Therefore, the control command exhibited a smoother transition than the initial control command, and the amplitude was smaller, which was easier to implement in engineering.

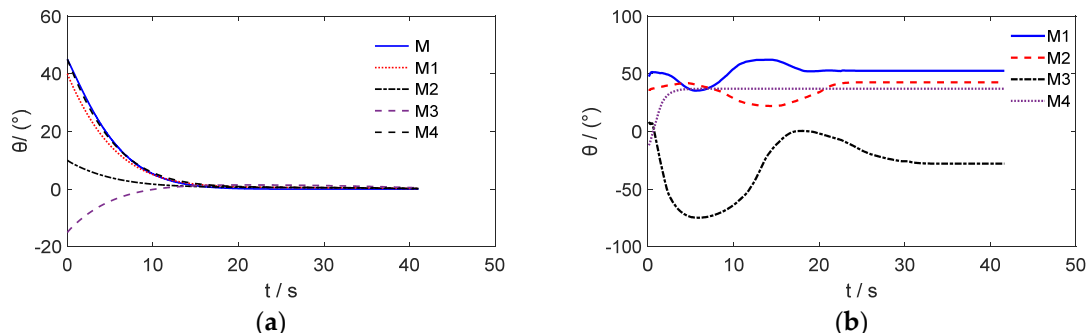


Figure 17. Comparison of the trajectory inclination curves of each follower missile between the proposed guidance scheme and the time cooperative guidance scheme: (a) Time cooperative guidance law; (b) MPC-based cooperative guidance law.

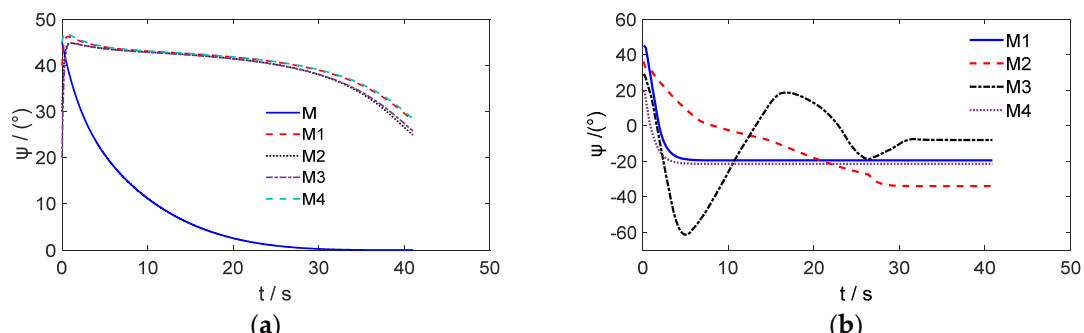


Figure 18. Comparison of the trajectory deflection curves of each follower missile between the proposed guidance scheme and the time cooperative guidance scheme: (a) Time cooperative guidance law; (b) MPC-based cooperative guidance law.

From Figures 19 and 20, it can be observed that the time cooperative guidance strategy required greater control capabilities, especially at the terminal. In order to achieve the consistency requirements of the time cooperative guidance, a greater overload is required, and the required overload exceeded that which the missile can provide. Therefore, this method has very high requirements for the maneuverability of the missiles. In contrast with the MPC-based cooperative strategy, the control amount can be controlled within a certain range through the strategy of rolling optimization, and the requirements for the maneuverability of the missile are not high. Furthermore, it can not only achieve the time cooperation, but also achieve the requirements of impact angle at the terminal. Thus, it proved to be a better cooperative guidance strategy.

The results demonstrated that the cooperative strategy of tracking the distance between the missile and the target based on the dynamic inverse design was very effective. The MPC algorithm added the impact angle constraints based on the impact time constraints, thereby achieving good effects and a better guidance performance, along with an easy implementation of the instructions.

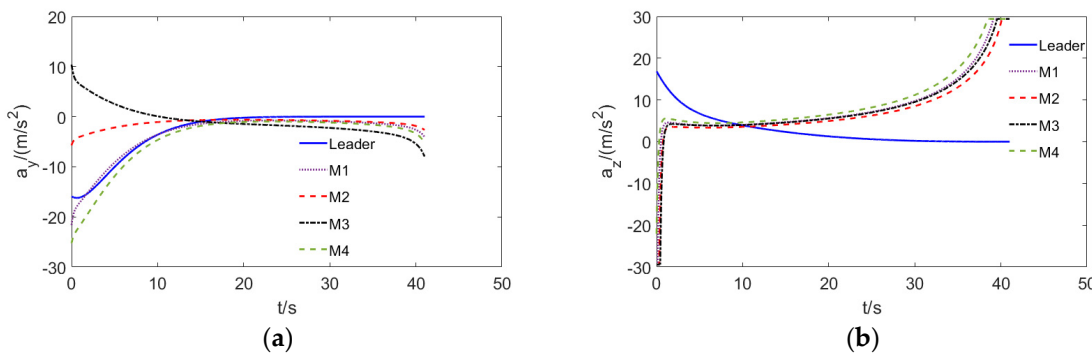


Figure 19. Normal acceleration curves obtained by the time cooperative guidance algorithm: (a) Normal acceleration curve of the dive plane; (b) Normal acceleration curve of turning plane.

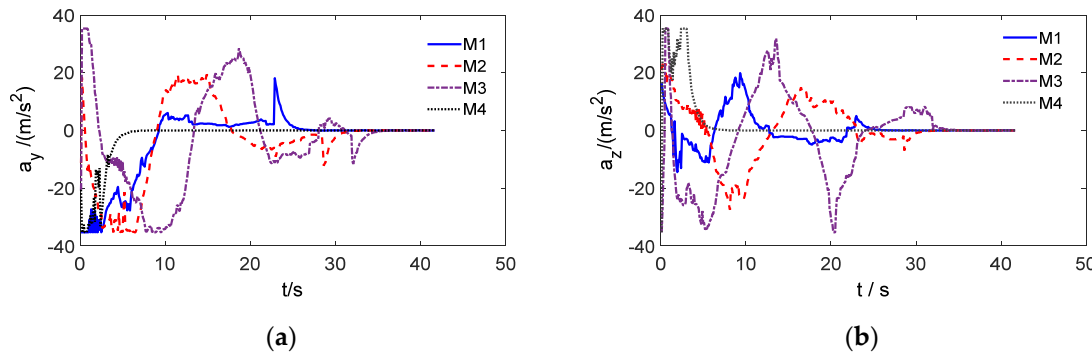


Figure 20. Normal acceleration curves obtained by the MPC guidance algorithm: (a) Normal acceleration curve of the dive plane; (b) Normal acceleration curve of turning plane.

6. Conclusions

In the present study, we proposed a three-dimensional cooperative terminal guidance strategy for cruise missiles under multiple constraints, introduced the concept of virtual leader missiles, and designed a cooperative strategy for the impact time of virtual leader and follower missiles. On this basis, using the model predictive control method, a three-dimensional cooperative guidance law was presented that could simultaneously control the multiple missiles with impact time and impact angle constraints on the premise of meeting the requirements of the miss distance. The algorithm implementation was carried out, and the effectiveness of the algorithm was verified using simulation studies. The robustness of the algorithm and the solution time of the algorithm both need further study in order to improve the operating efficiency of the algorithm and realize real-time calculations.

Author Contributions: Conceptualization, M.C. and X.C.; methodology, M.C. and Z.Z.; validation, Z.Z. and Z.L.; formal analysis, X.C. and Z.Z.; data curation, Z.L.; writing—original draft preparation, Z.Z. and Z.L.; writing—review and editing, M.C. All authors have read and agreed to the published version of the manuscript.

Funding: This research received no external funding.

Institutional Review Board Statement: Not applicable.

Informed Consent Statement: Not applicable.

Data Availability Statement: Not applicable.

Conflicts of Interest: The authors declare no conflict of interest.

References

1. Zhao, Q.; Dong, X.; Liang, Z.; Bai, C.; Chen, J.; Ren, Z. Distributed cooperative guidance for multiple missiles with fixed and switching communication topologies. *Chin. Aeronaut.* **2017**, *30*, 1570–1581. [[CrossRef](#)]
2. Nikusokhan, M.; Nobahari, H. Closed-form optimal cooperative guidance law against random step maneuver. *IEEE Trans. Aerosp. Electron. Syst.* **2016**, *52*, 319–336. [[CrossRef](#)]
3. Chen, P.; Xing, L.; Wu, S.-T.; Li, M. Concensus problems in distributed cooperative terminal guidance time of multi-missiles. *Control Decis.* **2010**, *25*, 1557–1561. (In Chinese)
4. Wang, L.; Ma, G.; Jiao, Y. Guidance law design of multi-aircraft formation cooperative interception with Angle constraint. *Nav. Aeronaut. Astronaut. Univ.* **2018**, *33*, 289–296. (In Chinese)
5. Li, G.; Yu, Z.; Zhang, Y. Cooperative guidance law with angle constraint to intercept maneuvering target. *Syst. Eng. Electron.* **2019**, *41*, 626–635. (In Chinese)
6. Zhao, B.; Huang, X.; Zhou, J.; Guo, Y. Multi-missile Distributed LOS Cooperative Guidance Law Designed Based on Sliding Mode Control. *Air Space Def.* **2020**, *3*, 16–23. (In Chinese)
7. Wang, Q.; Liu, M.; Ren, J.; Wang, T. Overview of Common Algorithms for UAV Path Planning. *J. Jilin Univ. (Inf. Sci. Ed.)* **2019**, *37*, 58–67. (In Chinese)
8. Wang, X.; Zheng, Y.; Lin, H. Integrated guidance and control law for cooperative attack of multiple missiles. *Aerosp. Sci. Technol.* **2015**, *42*, 1–11. [[CrossRef](#)]
9. Ates, U.H. Nonlinear impact angle control guidance law for stationary targets. In Proceedings of the AIAA Guidance, Navigation, and Control Conference, San Diego, CA, USA, 4–8 January 2016; pp. 2016–2112.
10. Gu, Y. Guidance Law of Multi-Missiles Formation Fight. *Mod. Def. Technol.* **2014**, *42*, 51–56. (In Chinese)
11. Wang, X.; Wang, J. Partial integrated guidance and control with impact angle constraints. *J. Guid. Control Dyn.* **2014**, *37*, 644–657. [[CrossRef](#)]
12. Tekin, R.; Erer, K.S. Switched-gain guidance for impact angle control under physical constraints. *J. Guid. Control Dyn.* **2015**, *38*, 205–216. [[CrossRef](#)]
13. Jeon, I.S.; Lee, J.I.; Tahk, M. Impact-time-control guidance law for anti-ship missiles. *IEEE Trans. Control Syst. Technol.* **2006**, *14*, 260–266. [[CrossRef](#)]
14. Yang, Z.; Lin, D.; Wang, H. Impact time control guidance law with field-of-view limit. *Syst. Eng. Electron.* **2018**, *38*, 2122–2128. (In Chinese)
15. Zhao, Q.L.; Chen, J.; Dong, X.W.; Wang, R.; Li, Q.D.; Zhang, R. Cooperative guidance law for heterogeneous missiles intercepting hypersonic weapon. *Acta Aeronaut. Astronaut. Sin.* **2016**, *37*, 936–948. (In Chinese)
16. Ye, P.; Zhang, J.; Li, Y.; Qi, G.; Sheng, D. Distributed cooperative guidance for multiple missiles with different line of sight Angle constraints. *Acta Armamentarll* **2019**, *40*, 506–515. (In Chinese)
17. Jeon, I.S.; Lee, J.I. Impact-time-control guidance law with constraints on seeker look angle. *IEEE Trans. Aerosp. Electron. Syst.* **2017**, *53*, 2621–2672. [[CrossRef](#)]
18. Chen, X.; Wang, J. Nonsingular sliding-mode control for field-of-view constrained impact time guidance. *J. Guid. Control Dyn.* **2018**, *41*, 1214–1222. [[CrossRef](#)]
19. Guo, Y.; Wang, H. Overview of cultural algorithms. *Comput. Eng. Appl.* **2009**, *45*, 41–46. (In Chinese)
20. Cho, N.; Kim, Y. Modified pure proportional navigation guidance law for impact time control. *J. Guid. Control Dyn.* **2016**, *39*, 852–872. [[CrossRef](#)]
21. Kang, S.; Kim, H. Differential game missile guidance with impact angle and time constraints. *IFAC Proc. Vol.* **2011**, *44*, 3920–3925. [[CrossRef](#)]
22. Erer, K.S.; Tekin, R. Impact time and angle control based on constrained optimal solutions. *J. Guid. Control Dyn.* **2016**, *39*, 2448–2454. [[CrossRef](#)]
23. Harl, N.; Balakrishnan, S.N. Impact time and angle guidance with sliding mode control. *IEEE Trans. Control Syst. Technol.* **2012**, *20*, 1436–1449. [[CrossRef](#)]

24. Kim, T.H.; Lee, C.H.; Jeon, I.S.; Tahk, M.J. Augmented polynomial guidance with impact time and angle constraints. *IEEE Trans. Aerosp. Electron. Syst.* **2013**, *49*, 2806–2817. [[CrossRef](#)]
25. Padhi, R.; Kothari, M. Model predictive static programming: A computationally efficient technique for suboptimal control design. *Int. J. Innov. Comput. Inf. Control* **2009**, *5*, 399–411.
26. Wang, J.; Li, F.; Zhao, J.; Wan, C. Review of multi-missile cooperative guidance law. *Flight Mechan.* **2011**, *29*, 13–18. (In Chinese)
27. Wang, X.; Hong, X.; Lin, H. A Method of Controlling Time and Impact Angle of Multiple-missiles Cooperative Combat. *J. Ballist.* **2012**, *24*, 1–5. (In Chinese)
28. Wang, Z.; Wang, X.; Lin, H. A Cooperative Guidance Law with Constraints of Impact Time and Impact Angle. *J. Ballist.* **2017**, *29*, 1–8. (In Chinese)
29. Song, J.; Song, S.; Xu, S. Multi-missile cooperative guidance law with Angle of attack constraint. *J. Chin. Inert. Technol.* **2016**, *24*, 554–560. (In Chinese)
30. Zhang, C.; Song, J.; Hou, B.; Zahng, M. Cooperative Guidance Law with Impact Angle and Impact Time Constraints for Networked Missiles. *Acta Armamentarill* **2016**, *37*, 431–438. (In Chinese)
31. Li, W.; Li, H.; Wang, L.; Gao, J. Design of Three-dimensional Guidance Law for Missiles Cooperative Engagement with Multiple Constraints. *Aerosp. Control* **2018**, *36*, 12–19. (In Chinese)
32. Slnai, E.; Lovera, M. Magnetic spacecraft attitude control: A survey and some new results. *Control Eng. Pract.* **2005**, *13*, 357–371.
33. Elsisi, M.; Ebrahim, M.A. Optimal design of low computational burden model predictive control based SSDA towards autonomous vehicle under vision. *Int. J. Intell. Syst.* **2021**, *26*, 6969–6987. [[CrossRef](#)]
34. Elsisi, M. Optimal design of nonlinear model predictive controller based on new modified multitracker optimization algorithm. *Int. J. Intell. Syst.* **2020**, *35*, 1857–1878. [[CrossRef](#)]
35. Shamaghdari, S.; Nikravesh, S.K.Y.; Haeri, M. Integrated guidance and control of elastic flight vehicle based on Robust MPC. *Int. J. Robust Nonlinear Control* **2015**, *25*, 2608–2630. [[CrossRef](#)]
36. Yao, Y.; Yang, B.; He, F.; Qiao, Y.; Cheng, D. Attitude control of missile via fliess expansion. *IEEE Trans. Control Syst. Technol.* **2008**, *16*, 959–970. [[CrossRef](#)]